

# Synthesis of Crystalline Nanosized $\alpha$ -Hafnium $\alpha$ -Hafnium-Titanium Phosphates from Crystallization of Their Parent Glassy Sodium Forms Via HF Solution and their Polystyrene Nanocomposite Membranes

**S. K. Shakshooki\***

Department of Chemistry, Faculty of Science, University of Tripoli, Tripoli, Libya

**R. M. Aleab**

Department of Chemistry, Faculty of Science, University of Tripoli, Tripoli, Libya

**N. A. Guima**

Department of Chemistry, Faculty of Science, University of Tripoli, Tripoli, Libya

## Abstract

Glassy hafnium-, hafnium-titanium phosphates,  $\text{Hf}(\text{HPO}_4)_2 \cdot 3\text{H}_2\text{O}$ ,  $\text{Hf}_x\text{Ti}_{(1-x)}(\text{HPO}_4)_2 \cdot 3\text{H}_2\text{O}$ , respectively, (where  $x = 0.9, 0.67, 0.50$ ) were prepared and characterized. Found to be amorphous with vitreous visual look. Crystalline layered nanosized  $\text{Hf}(\text{HPO}_4)_2 \cdot \text{H}_2\text{O}(\text{nHfP})$ ,  $\text{Hf}_x\text{Ti}_{(1-x)}(\text{HPO}_4)_2 \cdot \text{H}_2\text{O}(\text{nHfTiP})$ , where ( $x = 0.9, 0.67, 0.50$ ) were prepared from crystallization of their parent glassy sodium forms with HF solution in Pyrex round bottom flask. Size particles of (nHfP) and (nHfTiP) were calculated from XRD broadening method using the Scherer's equation, found to be 10.15, 18.69, 18.69, 16.92 nm, respectively. They were characterized by chemical, thermal, XRD analysis and Fourier transform spectroscopy (FT-IR). Their exchange capacities were determined. We think these materials crystallized during the conversion process in two steps: 1st their parent glassy sodium forms dissolved in HF solution forming a mixing complex, 2nd the crystalline products were gradually precipitated due to HF solution action on the Pyrex flask and to a certain extent evaporation of excess HF. Preparations of polystyrene/(nHfP)-, (nHfTiP) nanocomposite membranes were carried out by mixing slurry tetrahydrofuran (THF) solution of (nHfP)-, (nHfTiP) of different weight percentages (10, and 20 wt %), with THF solution of 5% polystyrene (PS) in concentration at 45°C with stirring for 48 hours. The resultant mixtures were poured into flat surface containers of desired thickness, respectively, and allowed to dry in air. The resultant fully dried composites were peeled from the glass containers. The composite membranes were transparent flexible thin films and were characterized by XRD, TGA and FT-IR.

**Keywords:** Polystyrene;  $\alpha$ - $\text{Hf}(\text{HPO}_4)_2 \cdot \text{H}_2\text{O}$ ;  $\alpha$ - $\text{Hf}_x\text{Ti}_{(1-x)}(\text{HPO}_4)_2 \cdot \text{H}_2\text{O}$ ; Nano composite membranes.



CC BY: [Creative Commons Attribution License 4.0](https://creativecommons.org/licenses/by/4.0/)

## 1. Introduction

Layered inorganic ion exchange materials of tetravalent metal phosphates are very insoluble compounds with good thermal stabilities, and possess high ion exchange capacities. Increase attention directed toward electrical conductance [1], and sensors [2]. Their layered crystalline materials, resemblance clay minerals [3].

Inorganic layered nanomaterials are receiving great attention because of their size, structure, and possible biochemical applications [4], that have been proven to be good carriers for organic polar molecules. Examples of these are zirconium phosphates [5], taking advantage of the expandable interlayer space of the layered materials. Researchers have been capable of encapsulating functional biomolecules into these inorganic matrices protecting them from interacting with environment, avoiding denaturation and enhancing their shelf [4, 6]. Nanoscaled tetravalent metal phosphates and their organic polymer composites comprise an important class of synthetic engineering. However, research in such area is still in its infancy [7-10]. Nanotechnologies are at the center of numerous investigations and huge investments.

Organic-inorganic nanocomposite membranes have gained great attention recently [9, 10]. The composite material may combine the advantage of each material, for instance, flexibility, processability of polymers and the selectivity and thermal stability of the inorganic filler [9-12].

The most studies on organic polymers composite with tetravalent metal phosphates were polyaniline, polypyrrole, poly(vinylalcohol), SPEEK and epoxy resin. [13-17].

Polystyrene (PS) is one of the most widely used thermoplastics in many fields, such as electrical appliances, packaging and building materials [18], because of its low cost, rigidity, highly transparencies and chemical stability. Yet, the applications of PS are also limited due to its poor thermal stability and mechanical property.

Generally polymer/ layered inorganic nanocomposites can be synthesized by various methods, including solution intercalation, in situ polymerization, solvothermal method or melt intercalation. Among these methods, solution intercalation is an extensively used, by which the polymer molecule can be directly introduced into the gallery of layered inorganic [18].

This paper describes the preparation and characterization of novel nanosized layered  $\alpha$ -hafnium-,  $\alpha$ -hafnium-titanium phosphates and their polystyrene nanocomposite membranes.

\*Corresponding Author

## 2. Materials and Methods

### 2.1. Chemicals

HfCl<sub>4</sub>, Polystyrene(PS) of Aldrich , TiCl<sub>4</sub>, H<sub>3</sub>PO<sub>4</sub> (85%) of BDH, HF (40% ) of Reidel De-Haen . Other chemicals used were of analytical grade.

### 2.2. Preparation of Glassy Hf (HPO<sub>4</sub>)<sub>2</sub>.3H<sub>2</sub>O

25 ml 0.5M HfCl<sub>4</sub> in 4M HCl, were added to 60ml 12% H<sub>3</sub>PO<sub>4</sub> with stirring at room temperature for 2hours. Then left to age in its mother liqueur for 48 hours, filtered, washed with distilled water up to pH=3. The resultant gel dried at 60°C, cracked with distilled water, filtered to obtain glassy (vitreous look) Hf (HPO<sub>4</sub>)<sub>2</sub>.3H<sub>2</sub>O.]

### 2.3. Preparation of Glassy Hafnium-Titanium Phosphates, Hf<sub>x</sub>Ti<sub>(1-x)</sub> (HPO<sub>4</sub>)<sub>2</sub>.3H<sub>2</sub>O

Typically: glassy Hf<sub>0.9</sub>Ti<sub>0.1</sub>(HPO<sub>4</sub>)<sub>2</sub>.3H<sub>2</sub>O preparation was carried out by mixing 20 ml 0.5M HfCl<sub>4</sub> and 2ml of 0.5M TiCl<sub>4</sub> in 4M HCl at room temperature . The resultant mixture was added drop wise to 60 ml 12% H<sub>3</sub>PO<sub>4</sub> with stirring at room temperature for 2hours. Then left to age in its mother liqueur for 48 hours, the resultant gel was filtered, washed up to pH=3, dried at 60°C, cracked with distilled water , then filtered, to obtain glassy (vitreous look) Hf<sub>0.9</sub>Ti<sub>0.1</sub>(HPO<sub>4</sub>)<sub>2</sub>.3H<sub>2</sub>O. In similar manner glassy Hf<sub>0.67</sub>Ti<sub>0.33</sub> (HPO<sub>4</sub>)<sub>2</sub>.3H<sub>2</sub>O and glassy Hf<sub>0.50</sub>Ti<sub>0.50</sub>(HPO<sub>4</sub>)<sub>2</sub>.3H<sub>2</sub>O, were prepared putting in consideration stoichiometric mixing of HfCl<sub>4</sub> and TiCl<sub>4</sub> solutions.

### 2.4. Preparation of Sodium form of Glassy Hafnium Phosphate, Hf(NaPO<sub>4</sub>)<sub>2</sub>.nH<sub>2</sub>O

0.3g of Hf(HPO<sub>4</sub>)<sub>2</sub>.3H<sub>2</sub>O was dispersed in 60 ml 0.1M NaCl solution, with stirring for an hour, to that 0.1M NaOH solution was added drop wise till pH of the solution = 8. The stirring was continued for half an hour, then filtered washed with distilled water, and left to dry in air.

### 2.5. Preparation of Sodium forms Glassy Hafnium-Titanium Phosphates, Hf<sub>0.5</sub>Ti<sub>0.5</sub> (NaPO<sub>4</sub>)<sub>2</sub>.nH<sub>2</sub>O

0.2g of Hf<sub>0.5</sub> Ti<sub>0.5</sub>(HPO<sub>4</sub>)<sub>2</sub>.3H<sub>2</sub>O(was dispersed in 40 ml 0.1M NaCl solution, with stirring for an hour, to that 0.1M NaOH solution was added drop wise till pH of the solution =8. The stirring was continued for half an hour, then filtered washed with distilled water, and left to dry in air.

### 2.6. Preparation of Sodium Forms Glassy Hafnium Titanium Phosphates Hf<sub>x</sub>Ti<sub>(1-x)</sub> (NaPO<sub>4</sub>)<sub>2</sub>.nH<sub>2</sub>O, (Where X=0.9 , 0.67)

0.8g of Hf<sub>x</sub> Ti<sub>(1-x)</sub> (HPO<sub>4</sub>)<sub>2</sub>.3H<sub>2</sub>O was dispersed in 160 ml 0.1M NaCl solution, with stirring for an hour, to that 0.1M NaOH solution was added drop wise till pH of the solution =8. The stirring was continued for half an hour, then filtered washed distilled water, and left to dry in air.

### 2.7. Crystallization of Sodium forms of Glassy Hafnium Phosphate, Hf(NaPO<sub>4</sub>)<sub>2</sub>.nH<sub>2</sub>O, and Glassy Hafnium-Titanium Phosphates , Hf<sub>x</sub> Ti<sub>(1-x)</sub> (NaPO<sub>4</sub>)<sub>2</sub>.nH<sub>2</sub>O, (Where X=0.9, 0.67, 0.5, n = 3-4H<sub>2</sub>O)

#### 2.7.1. Crystallization of Sodium Form of Glassy Hafnium Phosphate

0.2g of Hf(NaPO<sub>4</sub>)<sub>2</sub>.nH<sub>2</sub>O was dissolved in 12ml of 6M HF solution in plastic container, then transferred to Pyrex round bottle flak , volume 100ml, closed with parafilm and left at room temperature for 4 days, the resultant ppt. was filtered, washed with distilled water, and left to dry in air.

#### 2.7.2. Crystallization of Sodium Form of Glassy Hf<sub>0.5</sub>Ti<sub>0.5</sub> (NaPO<sub>4</sub>)<sub>2</sub>.nH<sub>2</sub>O

0.2g of Hf<sub>0.5</sub>Ti<sub>0.5</sub>(NaPO<sub>4</sub>)<sub>2</sub>.nH<sub>2</sub>O was dissolved in 12ml of 7M HF solution in plastic container, then transferred to Pyrex round bottle flak , volume 100ml, closed with parafilm and left at room temperature for 4 days, the resultant ppt. was filtered, washed with distilled water, and left to dry in air.

#### 2.7.3. Crystallization of Sodium Forms of Glassy Hafnium-Titanium Phosphates Hf<sub>x</sub>Ti<sub>(1-x)</sub> (NaPO<sub>4</sub>)<sub>2</sub>.nH<sub>2</sub>O

0.8g of glassy hafnium-titanium phosphates, Hf<sub>x</sub>Ti<sub>(1-x)</sub>(NaPO<sub>4</sub>)<sub>2</sub>.nH<sub>2</sub>O, (x= 0.9, 0.67) were dissolved in 50 ml of 6M HF solution in plastic container, then each transferred into Pyrex round bottle flak , volume 100ml, closed with parafilm and left at room temperature for 4 days, the resultant ppts, filtered, washed with distilled water, and left to dry in air.

### 2.7.4. Determination of the Exchange Capacities of the Resultant Crystalline Layered $\alpha$ -Hf ( $\text{HPO}_4$ )<sub>2</sub>·H<sub>2</sub>O and $\alpha$ -Hf<sub>x</sub>Ti<sub>(1-x)</sub> ( $\text{HPO}_4$ )<sub>2</sub>·H<sub>2</sub>O.

To 100mg of the resultant crystalline layered phosphates, 25ml of 0.1M NaCl were added, stirred vigorously for 1hr, then titrated with 0.1M NaOH. Their exchange capacities found to be equal to 2/their molecular weights (in Meq/g).

### 2.7.5. Preparation of 5%Polystyrene(PS) Solution

Polystyrene(PS) in 5 %concentration was prepared by dissolving 10g of PS in 200 ml tetrahydrofuran (THF) at ~ 25°C.

### 2.8. Preparation of PS/ Crystalline Layered $\alpha$ -Hf ( $\text{HPO}_4$ )<sub>2</sub>· H<sub>2</sub>O (nHfP) and $\alpha$ -Hf<sub>x</sub> Ti<sub>(1-x)</sub> ( $\text{HPO}_4$ )<sub>2</sub>· H<sub>2</sub>O (nHfTiP) Nano Composite Membranes

Different PS/ nHfP-, nHfTiP nanocomposite membranes were prepared where their weight % loading were (10, 20 % in wt).

Typically, preparation of PS/ nHfP (10% in wt) nanocomposite membrane:

0.1g of  $\alpha$ -Hf ( $\text{HPO}_4$ )<sub>2</sub>·H<sub>2</sub>O was dispersed in 5ml THF, with stirring for 1hr, to that 18 ml polystyrene solution (5% in concentration) was added with vigorous stirring at room temperature for 30 min. The stirring was continued at 45°C for 48 h. The resultant mixture was poured into flat surface container, of desired thickness, and was allowed to dry in air. The fully dried transparent flexible thin film was peeled from the glass container to obtain PS/ nHfP nano composite(10% in wt). Similarly PS/nHfP(20% in wt) PS/nHfTiP (10,20% in wt) nano composite membranes were prepared using the required mixed ratios.

### 2.9. Instruments Used for Characterization

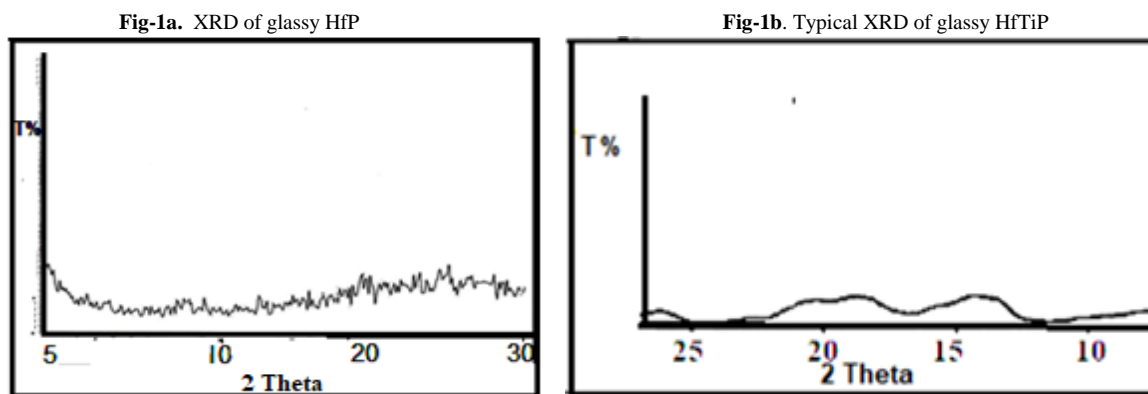
X-ray powder diffractometry Philips using Ni-filtered CuK $\alpha$  ( $\lambda = 1.54056\text{\AA}$ ), Thermal Analysis, TGA Perkin-ElmerSII, Fourier Transform IR spectrometer, model IFS25 Bruker25, pH Meter WGW 521.

## 3. Results and Discussion

Glassy hafnium-, hafnium- titanium Phosphates, Hf( $\text{HPO}_4$ )<sub>2</sub>·3H<sub>2</sub>O, Hf<sub>x</sub>Ti<sub>(1-x)</sub> ( $\text{HPO}_4$ )<sub>2</sub>·3H<sub>2</sub>O. They were characterized. Found to be amorphous with vitreous visual look, similar to that already reported by [Shakshooki, et al. \[19\]](#).

### 3.1. Typical XRD of Resultant Glassy HfP and HfTiP

The resultant glassy Hf( $\text{HPO}_4$ )<sub>2</sub>·3H<sub>2</sub>O(HfP), Hf<sub>x</sub>Ti<sub>(1-x)</sub> ( $\text{HPO}_4$ )<sub>2</sub>·3H<sub>2</sub>O (HfTiP), found to be amorphous. Figures (1a,1-b) show XRD pattern of the glassy HfP and Typical XRD of glassy HfTiP



### 3.2. XRD of the Resultant Crystalline Layered Nhfp, Nhtip

Crystalline layered  $\alpha$ -Hf( $\text{HPO}_4$ )<sub>2</sub>·H<sub>2</sub>O and Tailor made crystalline layered  $\alpha$ -Hf<sub>x</sub>Ti<sub>(1-x)</sub> ( $\text{HPO}_4$ )<sub>2</sub>·H<sub>2</sub>O ( $x=0.9, 0.67, 0.50$ ) were obtained with variable Ti-contents by novel method. These materials can be considered as ion exchangers, solid acid catalysts, intercalates, and as proton conductors.

Figures (2-5) show X-ray diffractogram patterns of the resultant novel crystalline layered nanosized  $\alpha$ -Hf( $\text{HPO}_4$ )<sub>2</sub>·H<sub>2</sub>O,  $\alpha$ -Hf<sub>x</sub>Ti<sub>(1-x)</sub> ( $\text{HPO}_4$ )<sub>2</sub>·H<sub>2</sub>O, that were obtained from conversion of their parent glassy sodium forms via HF solution. Evaluation of the X-ray curves based on the position of the first peaks showed that materials of  $\alpha$ -type layered crystalline structure. The materials are crystalline with good degree of crystallinity for the resultant crystalline  $\alpha$ -Hf( $\text{HPO}_4$ )<sub>2</sub>·H<sub>2</sub>O, and crystalline  $\alpha$ -Hf<sub>0.9</sub>Ti<sub>0.1</sub>( $\text{HPO}_4$ )<sub>2</sub>·H<sub>2</sub>O,  $\alpha$ -Hf<sub>0.67</sub>Ti<sub>0.33</sub> ( $\text{HPO}_4$ )<sub>2</sub>·H<sub>2</sub>O and  $\alpha$ -Hf<sub>0.5</sub>Ti<sub>0.5</sub>( $\text{HPO}_4$ )<sub>2</sub>·H<sub>2</sub>O, respectively, as is represented by sharpness of the peaks, show better crystallinity from those found earlier (with the same composition) that was prepared by the reflux method [20]. Their interlayer distance ( $d_{001}$ ) found to be in the range of 7.56 $\text{\AA}$  for  $\alpha$ -Hf( $\text{HPO}_4$ )<sub>2</sub>·H<sub>2</sub>O and 7.5 $\text{\AA}$ , for crystalline layered  $\alpha$ -Hf<sub>x</sub>Ti<sub>(1-x)</sub> ( $\text{HPO}_4$ )<sub>2</sub>·H<sub>2</sub>O.

**Fig-2.** XRD of  $\alpha$ -HfP(HPO<sub>4</sub>)<sub>2</sub>.H<sub>2</sub>O.

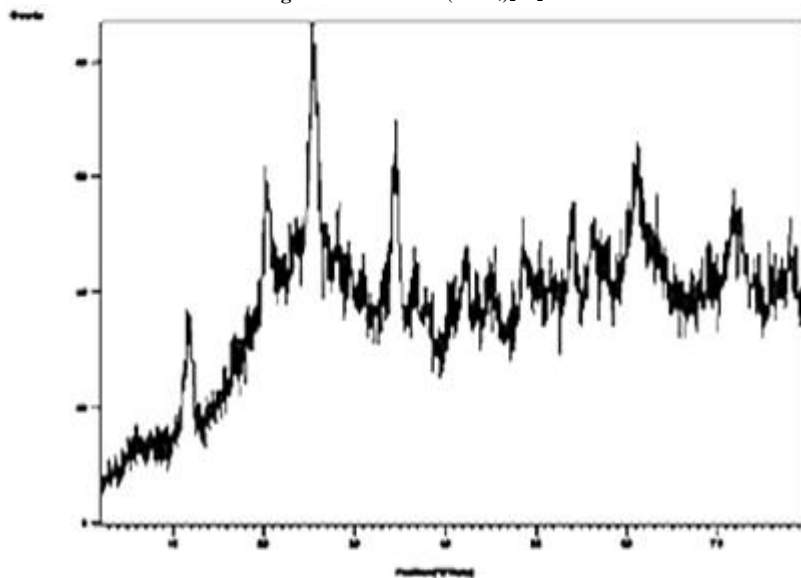


**Fig-3-** XRD of  $\alpha$ -Hf<sub>0.9</sub>Ti<sub>0.1</sub>(HPO<sub>4</sub>)<sub>2</sub>.H<sub>2</sub>O

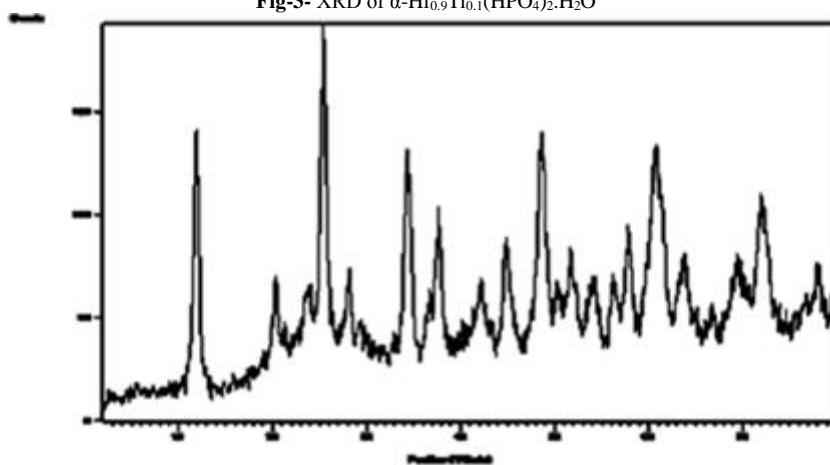


**Fig-4.** XRD of  $\alpha$ -Hf<sub>0.67</sub>Ti<sub>0.33</sub>(HPO<sub>4</sub>)<sub>2</sub>.H<sub>2</sub>O.

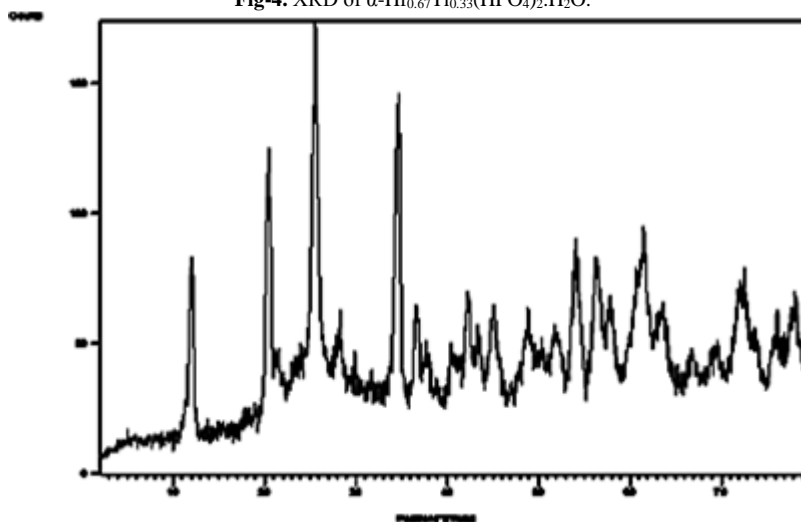
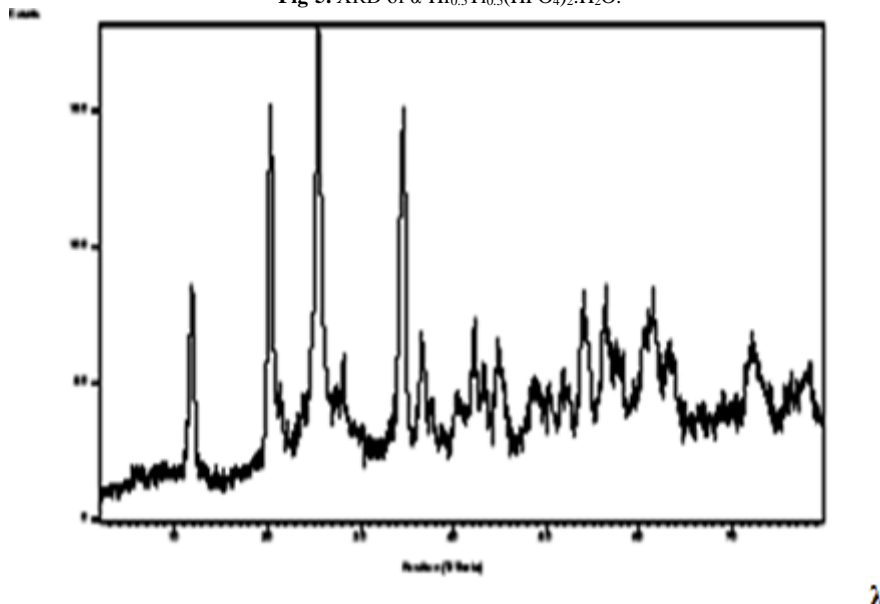


Fig-5. XRD of  $\alpha$ -Hf<sub>0.5</sub>Ti<sub>0.5</sub>(HPO<sub>4</sub>)<sub>2</sub>.H<sub>2</sub>O.

The average diameters of  $\alpha$ -Hf (HPO<sub>4</sub>)<sub>2</sub>.H<sub>2</sub>O,  $\alpha$ -Hf<sub>0.9</sub>Ti<sub>0.1</sub>(HPO<sub>4</sub>)<sub>2</sub>.H<sub>2</sub>O,  $\alpha$ -Hf<sub>0.67</sub>Ti<sub>0.33</sub>(HPO<sub>4</sub>)<sub>2</sub>.H<sub>2</sub>O,  $\alpha$ -Hf<sub>0.5</sub>Ti<sub>0.5</sub>(HPO<sub>4</sub>)<sub>2</sub>.H<sub>2</sub>O were found to be 10.15, 18.69, 18.69, 16.92 nm, respectively, which were calculated from the full width at half maximum of the peak using Scherer's equation [20].

$$D = \frac{0.9\lambda}{\beta \cos \theta_{\max}}$$

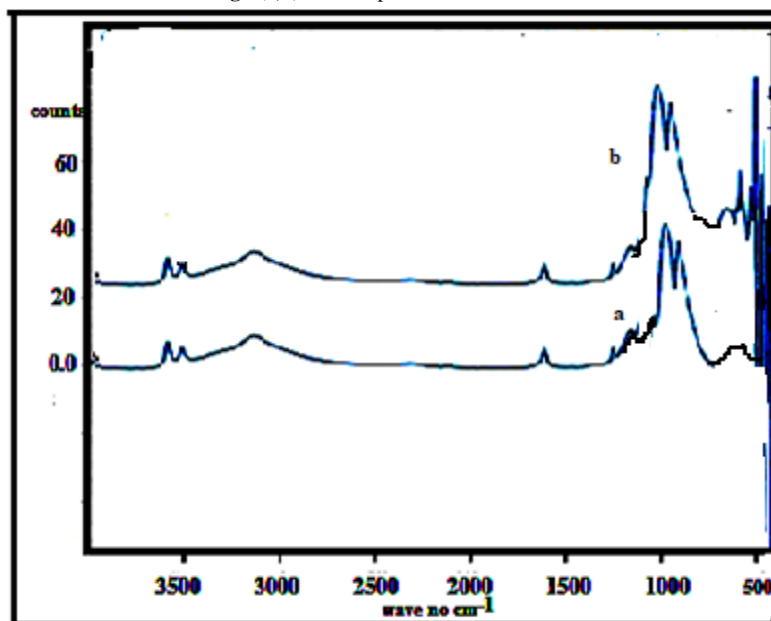
Where **D** is the average crystal size, **0.9** constant,  $\lambda$  is the characteristic wave length of x-ray used ( $\lambda=1.54056$  Å),  $\theta$  is the diffraction angle, and the  $\beta$  is the angular width in the radius at intensity equal to half of the maximum peak intensity [20].

### 3.3. FT-IR of the Resultant Crystalline Layered nHfP, nHfTiP

Vibration spectroscopy, together with diffractogram, allow the studying the chemical structure of a material as well as the modifications induced by physical and chemical process. In particular, infrared spectra becomes a key tool to investigated structures of tetravalent metal phosphates [21, 22].

Figure 6(a,b) shows FT-IR spectra of  $\alpha$ -Hf(HPO<sub>4</sub>)<sub>2</sub>.H<sub>2</sub>O and  $\alpha$ -Hf<sub>x</sub>Ti<sub>(1-x)</sub>(HPO<sub>4</sub>)<sub>2</sub>.H<sub>2</sub>O, respectively, in the range 4000-400cm<sup>-1</sup> wave number. They are almost identical. Broad band in the range 3535-2960cm<sup>-1</sup> centered at about 3131cm<sup>-1</sup> assigned to vibrational O-H asymmetric modes of interlayer water molecules. The band a about 1616cm<sup>-1</sup> corresponds to H-O-H bending modes. The strong broad band centered at about 1005cm<sup>-1</sup> is characteristic to the bonding in plane of the (P-O) bond of phosphate groups.

Fig-6(a,b). FT-IR spectrum of nHfP and nHTiP



Organic-inorganic hybrid materials, based on interactions between organic and inorganic components, have been greatly developed in the past decades. Among them, polymer nanocomposites consist of a polymer matrix and layered nano-fillers have gained a lot of interest when polymer and layered inorganic components are blended at the molecular level, many properties can be obviously improved, including mechanical properties, thermal stability.

### 3.4. PS/ nHfP, nHfTiP Composite Membranes

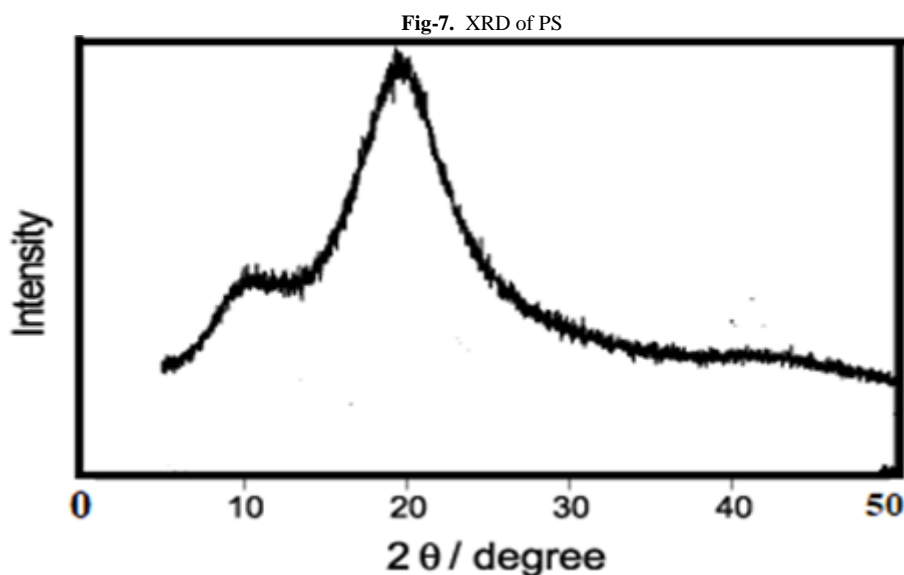
Flexible transparent thin films homogeneous composites of PS/ nHfP, nHTiP were prepared from mixing slurry THF solutions of nHfP, and of nHTiP different weight percentages (wt%) with THF solution of PS 5% in concentration at 45°C. The resultant composites were characterized by, X-ray, TGA and FT-IR spectra.

### 3.5. XRD of PS and PS/ nHfP, nHTiP Composites

Figures (7-11) show the XRD patterns of the PS, nHfP and nHfTiP nanocomposite membranes respectively.

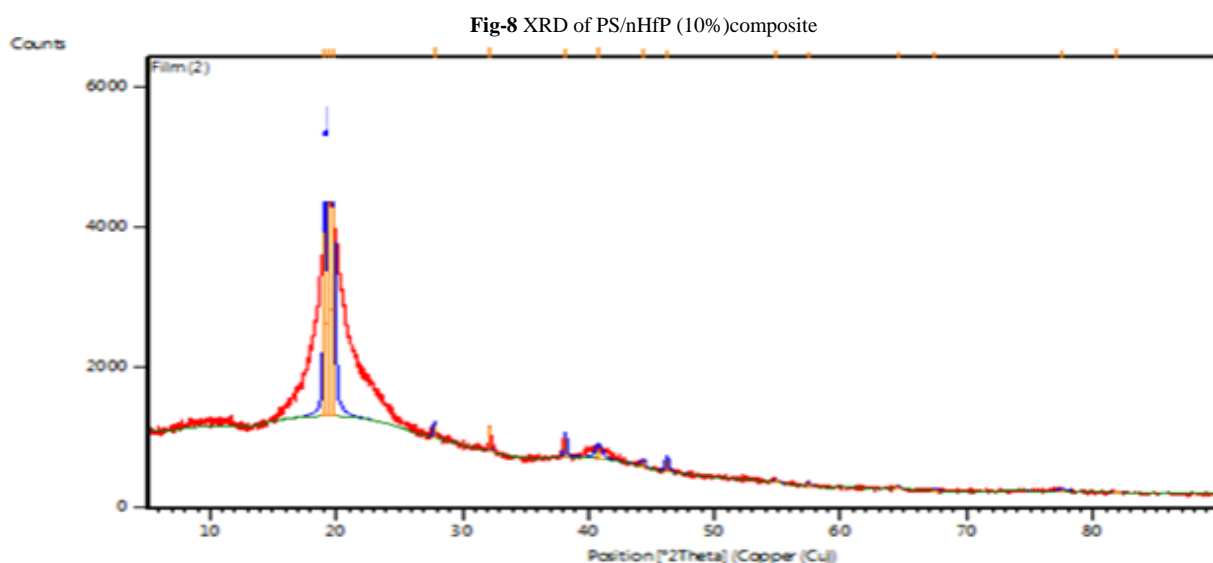
#### 3.5.1. XRD of PS

Figure 7 shows the XRD of the Polystyrene with intense peak appearing near  $2\theta = 21^\circ$ .



#### 3.5.2. XRD Ps/ of nHfP Nanocomposite Membrane

Figure 8 shows the XRD of PS/  $\text{Hf}(\text{HPO}_4)_2 \cdot \text{H}_2\text{O}$  nanocomposite membrane of 10% inorganic content consists of small broad peak at  $2\theta = 11.54^\circ$  where PS show broad peak centered at  $2\theta = 21.5^\circ$ , characteristics of HfP XRD and of layered PS, respectively. That indicate the formation of the PS composite.



#### 3.5.3. XRD of PS/ Nhftip Nanocomposite Membranes

Figure 9 shows the XRD of PS/  $\text{Hf}_{0.9}\text{Ti}_{0.1}(\text{HPO}_4)_2 \cdot \text{H}_2\text{O}$ -, nanocomposite membrane of 10% inorganic content, consists of small peak at  $2\theta = 11.6^\circ$  where PS show broad peak centered at  $2\theta = 21.7^\circ$ , characteristics of XRD layered  $\text{Zr}_{0.9}\text{Ti}_{0.1}\text{P}$  and of PS, respectively. That indicate the formation of the PS composite.

Figure 10 shows  $\text{Hf}_{0.67}\text{Ti}_{0.33}(\text{HPO}_4)_2 \cdot \text{H}_2\text{O}$  nanocomposite membranes of 10% inorganic content. with small peak at  $2\theta = 11.65^\circ$  where PS show broad peak centered at  $2\theta = 21.5^\circ$ , characteristics of XRD layered  $\text{Hf}_{0.67}\text{Ti}_{0.33}$  and of PS, respectively. That indicate the formation of the resultant PS composite.

Figure 11 shows  $\text{Hf}_{0.50}\text{Ti}_{0.50}(\text{HPO}_4)_2 \cdot \text{H}_2\text{O}$  nanocomposite membranes of 10% inorganic content, respectively. with small peak at  $2\theta = 11.7^\circ$  where PS show broad peak centered at  $2\theta = 22^\circ$ , characteristics of XRD layered  $\text{Hf}_{0.50}\text{Ti}_{0.50}\text{P}$  and of PS, respectively. That indicate the formation of the resultant PS composite.

Fig-9. XRD of PS/nHf<sub>0.9</sub>Ti<sub>0.1</sub>P(10%) composite

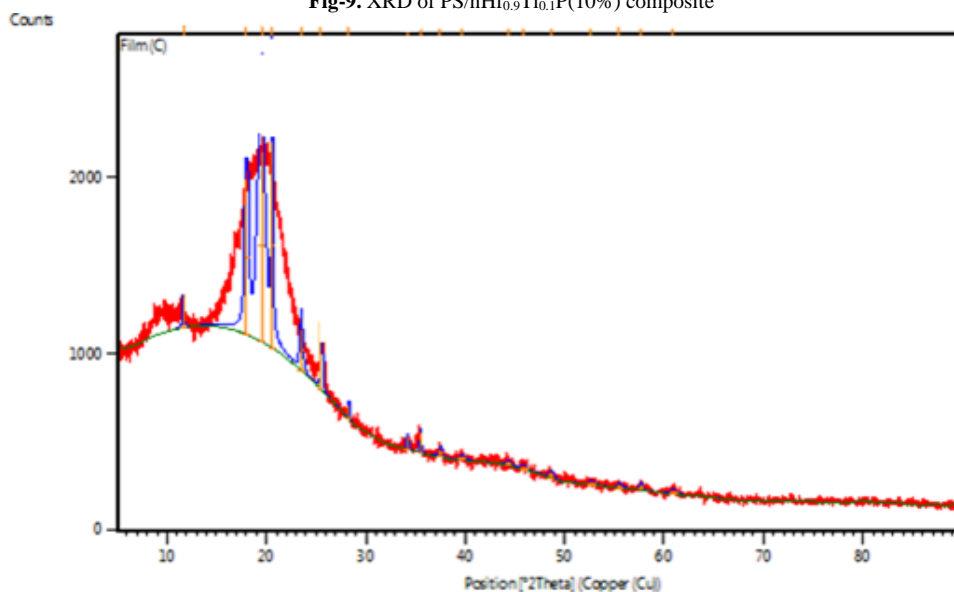


Fig-10. XRD of PS/nHf<sub>0.67</sub>Ti<sub>0.33</sub>P(10%) composite

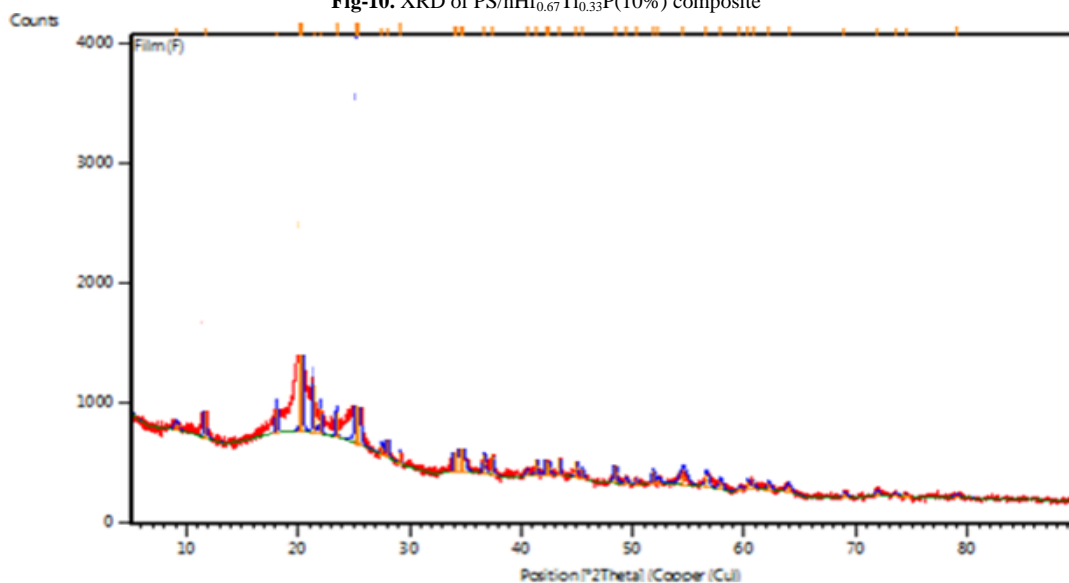
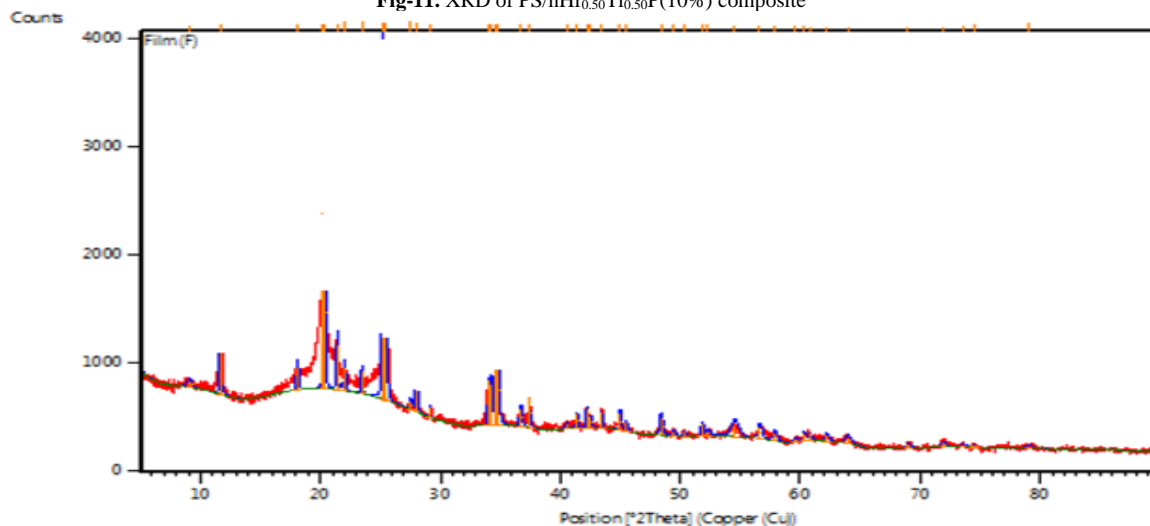


Fig-11. XRD of PS/nHf<sub>0.50</sub>Ti<sub>0.50</sub>P(10%) composite

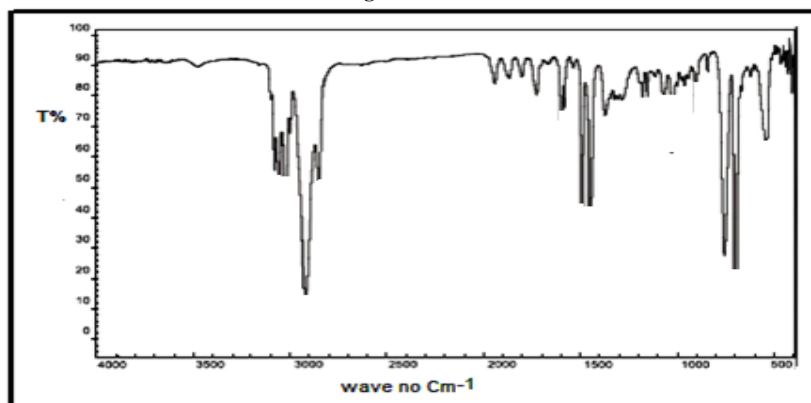




### 3.6. FT-IR of PS

Figure 12. show ands of the IR spectrum for polystyrene correspond to their functional groups, C-H aromatic tension  $3081,2\text{ cm}^{-1} - 3001,11\text{ cm}^{-1}$ ;  $2923,91\text{ cm}^{-1}$  and  $2850,40\text{ cm}^{-1}$   $\text{CH}_2$  asymmetric and symmetric tension;  $1943,19\text{ cm}^{-1}$ - $1728,23\text{ cm}^{-1}$  aromatic ring mono substitution;  $1452,28\text{ cm}^{-1}$  deformation  $\text{CH}_2 + \text{C}=\text{C}$  of the aromatic ring;  $1069,65\text{ cm}^{-1}$  flexion C-H in the plane.

Fig-12. FT-IR of PS



### 3.7. FT-IR Spectra of PS/Nhfp And PS/Nhtifp Nanocomposite Membrane

Figures (13,14) show the FT-IR spectra for polystyrene and PS/nHfP and PS/nHTiP nanocomposite membrane. Both spectra found to be almost identical. Broad band in the range  $3500\text{ cm}^{-1}$ - $3350\text{ cm}^{-1}$  assigned to vibration O-H asymmetric modes of interlayer water molecules. Bands in the range  $3081\text{ cm}^{-1}$ - $2850\text{ cm}^{-1}$  correspond to CH aromatic tension,  $\text{CH}_2$  ,asymmetric and symmetric tension. Bands in the range  $1943,19\text{ cm}^{-1}$ - $1728,23\text{ cm}^{-1}$  aromatic ring mono substitution;  $1452,28\text{ cm}^{-1}$  deformation  $\text{CH}_2 + \text{C}=\text{C}$  of the aromatic ring. The strong broad band centered at about  $1010\text{ cm}^{-1}$  is characteristic to the bonding in plane of the (P-O) bond of phosphate groups.

Fig-13. FT-IR spectrum of PS/nHfP

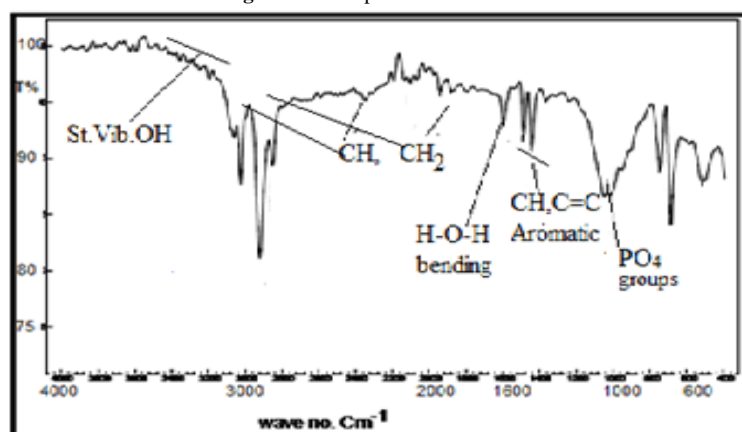
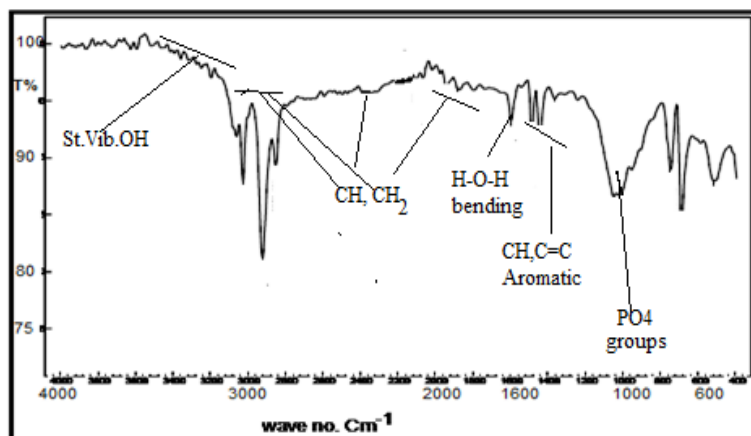


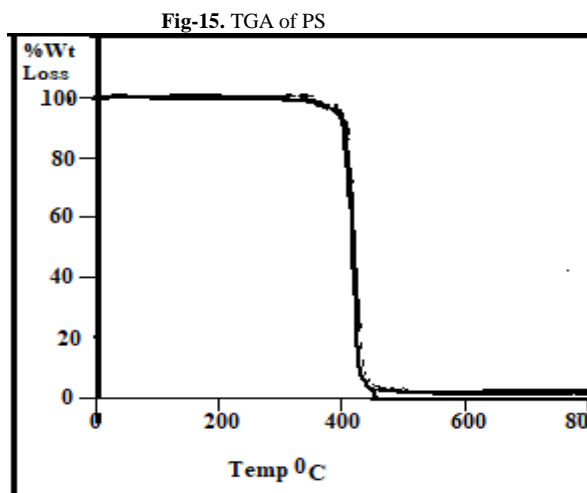
Fig-14. Typical FT-IR spectrum of PS/nHTiP





### 3.8. TGA of Polystyrene(PS)

Like all organic compounds, polystyrene burns to give carbon dioxide and water vapor. typically combusts incompletely. Thermogravimetric analysis of PS is shown in Figure 15. The thermal degradation of the polymer begins at 270 degrees Figure 13<sup>0</sup>C in air and stop at 425<sup>0</sup>C. The main groups of vaporized compounds generated were monoalkyl-substituted aromatic hydrocarbons and their oxidized products.



### 3.1. TGA of PS/ nHfP-, nHfTiP nanocomposite membranes

The TGA measurements of PS/nHfP-, nHfTiP nanocompsite membranes with inorganic contents (10, 20 % in wt) are shown in figures (16-19) , respectively. The thermal decomposition of the composite materials found to follow almost the same trend.

Thermal decomposition of composite membrane of PS/ nHfP (10% in wt) occurs in 3stages is given in Figure (16-a). First stage shows 7% weight loss up to 196°C, which may be due to the removal of external water molecules. The weight loss occurs between 196--715°C (the 2,3 stages) corresponds to the decomposition of PS and condensation of P-OH groups of the inorganic material to pyrophosphate , HfP<sub>2</sub>O<sub>7</sub>. The residue found to be around 4%.

Fig-16.a. TGAPS/nHfP(10%) composite membrane

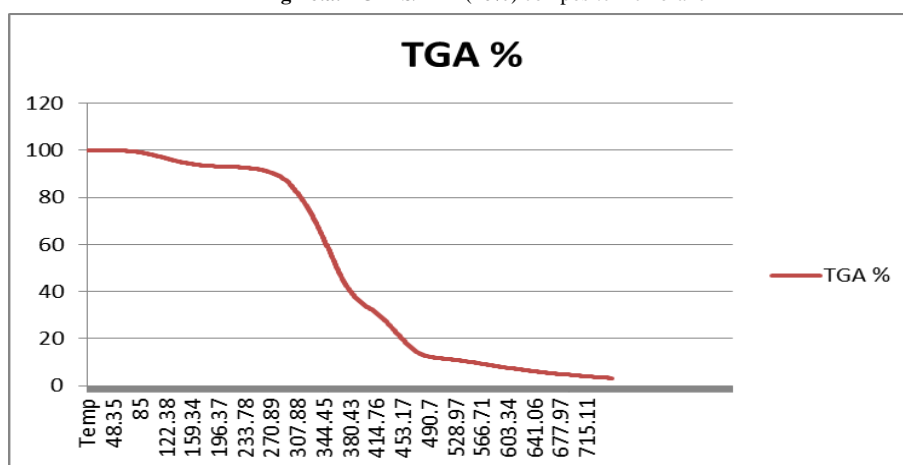


Fig-16.b. TGAPS/nHfP(20%) composite membrane

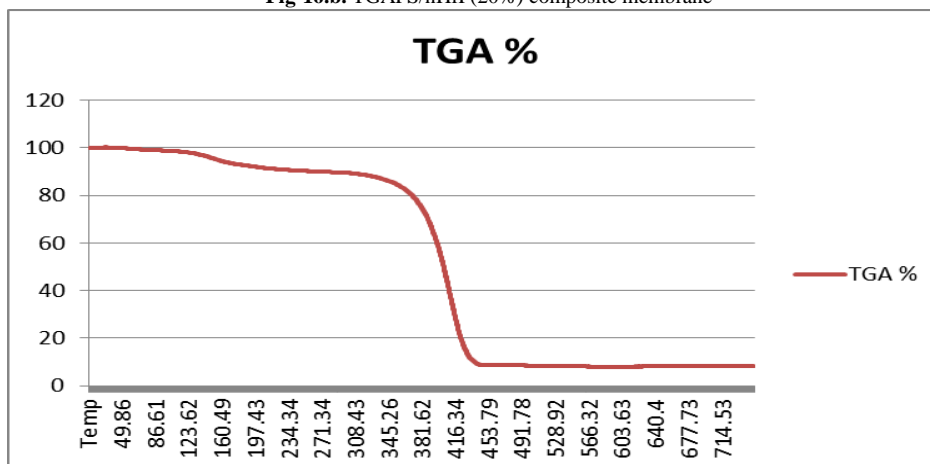
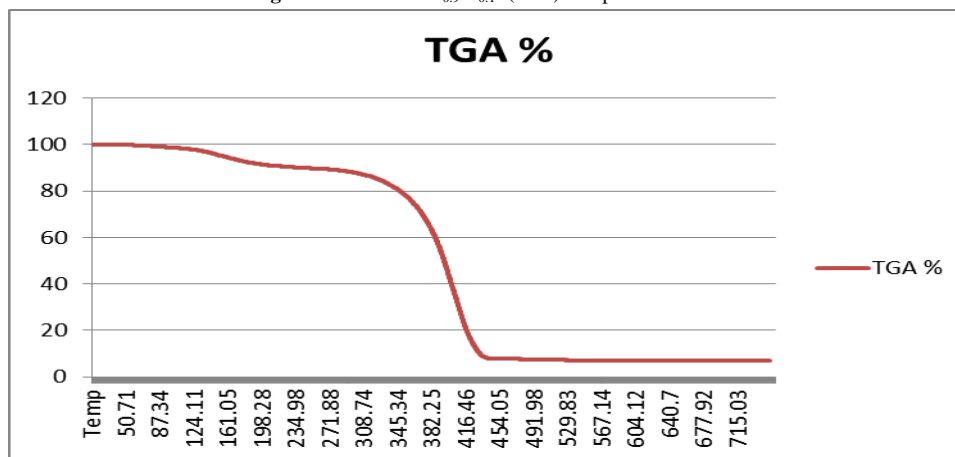


Figure (16-b) shows Thermal decomposition of composite membrane of PS/ nHfP (20% in wt) occurs in 2 stages. First stage shows 11% weight loss up to 271°C, which may be due to the removal of external water molecules. The weight loss occurs between 271-480°C (the 2nd stage) corresponds to the decomposition of PS and condensation of P-OH groups of the inorganic material to pyrophosphate,  $\text{HfP}_2\text{O}_7$ . The residue found to be around 9%.

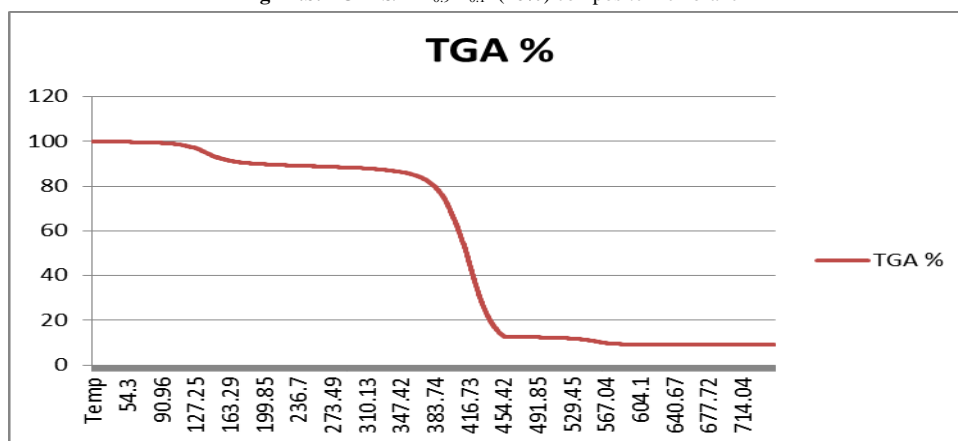
Thermal decomposition of composite membrane of PS/  $\text{nHf}_{0.9}\text{Ti}_{0.1}\text{P}$  (10% in wt) occurs in 2 stages is given in Figure (17-a) First stage shows 10% weight loss up to 290 °C, which may be due to the removal of external water molecules. The weight loss occurs between 290-529°C ( the 3 stages) corresponds to the decomposition of PS and condensation of P-OH groups of the inorganic material to pyrophosphate ,  $(\text{Hf}_{0.9}\text{Ti}_{0.1})\text{P}_2\text{O}_7$ . The residue found to be around 7%.

Fig-17.a. TGAPS/nHf<sub>0.9</sub>Ti<sub>0.1</sub>P(10%) composite membrane

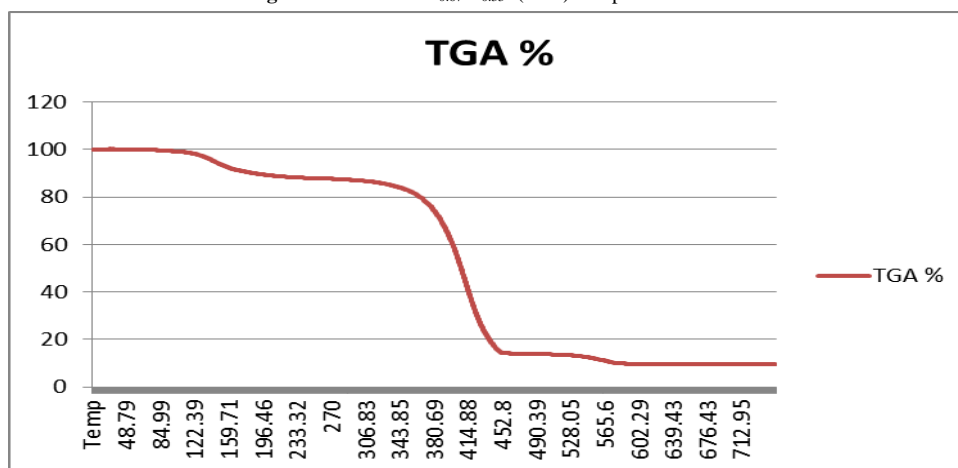


Thermal decomposition of composite membrane of PS/  $\text{nHf}_{0.9}\text{Ti}_{0.1}\text{P}$  (10% in wt) occurs in 3stages is given in Figure (17-b) First stage shows 11% weight loss up to 273 °C, which may be due to the removal of external water molecules. The weight loss occurs between 273-604 °C ( the 2 stages) corresponds to the decomposition of PS and condensation of P-OH groups of the inorganic material to pyrophosphate ,  $(\text{Hf}_{0.9}\text{Ti}_{0.1})\text{P}_2\text{O}_7$ . The residue found to be around 10%.

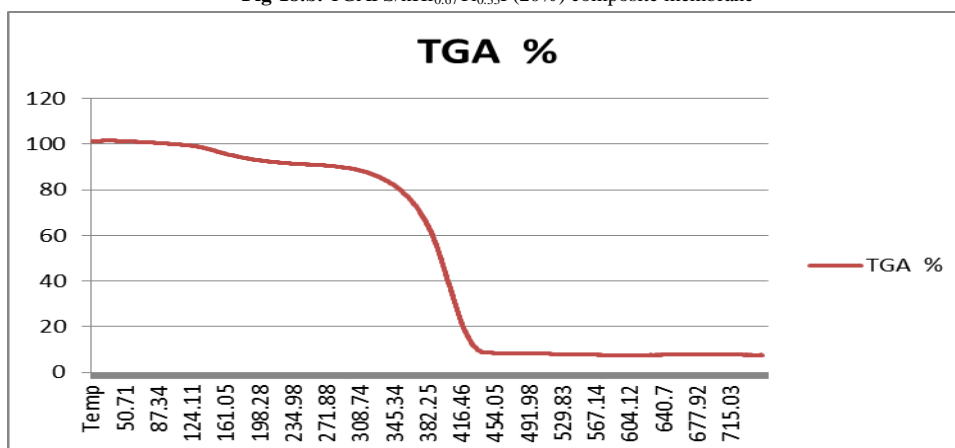
Fig-17.b. TGAPS/nHf<sub>0.9</sub>Ti<sub>0.1</sub>P(20%) composite membrane



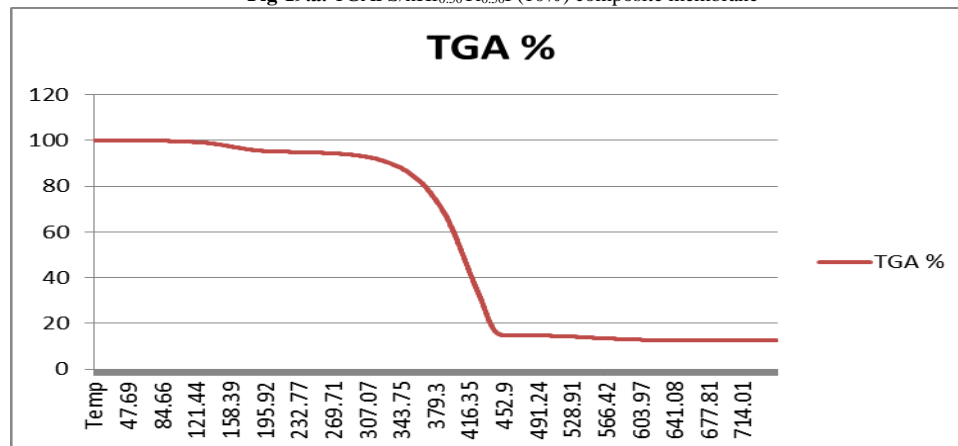
Thermal decomposition of composite membrane of PS/  $\text{nHf}_{0.67}\text{Ti}_{0.33}\text{P}$  (10% in wt) occurs in 3stages is given in Figure (18-a) First stage shows 11% weight loss up to 270 °C, which may be due to the removal of external water molecules. The weight loss occurs between 270-639 °C ( the 2 stages) corresponds to the decomposition of PS and condensation of P-OH groups of the inorganic material to pyrophosphate ,  $(\text{Hf}_{0.67}\text{Ti}_{0.33})\text{P}_2\text{O}_7$ . The residue found to be around 11%.

**Fig-18.a.** TGAPS/nHf<sub>0.67</sub>Ti<sub>0.33</sub>P(10%) composite membrane

Thermal decomposition of composite membrane of PS/ nHf<sub>0.67</sub>Ti<sub>0.33</sub>P (20% in wt) occurs in 2stages is given in Figure (18-b) First stage shows 9% weight loss up to 271 °C, which may be due to the removal of external water molecules. The weight loss occurs between 271-639 °C ( the corresponds to the decomposition of PS and condensation of P-OH groups of the inorganic material to pyrophosphate , (Hf<sub>0.67</sub>Ti<sub>0.33</sub>)P<sub>2</sub>O<sub>7</sub>. The residue found to be around 9%.

**Fig-18.b.** TGAPS/nHf<sub>0.67</sub>Ti<sub>0.33</sub>P(20%) composite membrane

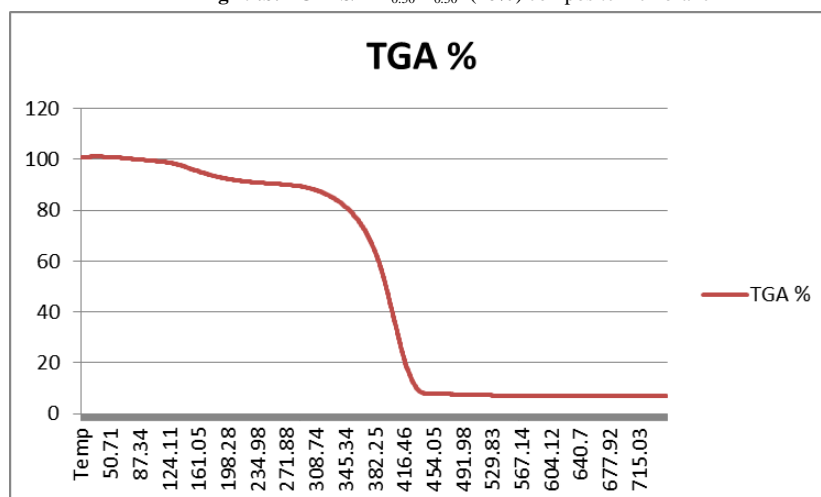
Thermal decomposition of composite membrane of PS/ nHf<sub>0.50</sub>Ti<sub>0.50</sub>P (10% in wt) occurs in 2stages is given in Figure (19-a) First stage shows 4% weight loss up to 269 °C, which may be due to the removal of external water molecules. The weight loss occurs between 269-603°C corresponds to the decomposition of PS and condensation of P-OH groups of the inorganic material to pyrophosphate , (Hf<sub>0.67</sub>Ti<sub>0.33</sub>)P<sub>2</sub>O<sub>7</sub>. The residue found to be around 13%.

**Fig-19.a.** TGAPS/nHf<sub>0.50</sub>Ti<sub>0.50</sub>P(10%) composite membrane

Thermal decomposition of composite membrane of PS/ nHf<sub>0.50</sub>Ti<sub>0.50</sub>P (20% in wt) occurs in 2stages is given in Figure (19-b) First stage shows 10% weight loss up to 271 °C, which may be due to the removal of external water

molecules. The weight loss occurs between 271-567°C corresponds to the decomposition of PS and condensation of P-OH groups of the inorganic material to pyrophosphate,  $(\text{Hf}_{0.67}\text{Ti}_{0.33})\text{P}_2\text{O}_7$ . The residue found to be around 6.5%.

Fig-19.b. TGAPS/nHf<sub>0.50</sub>Ti<sub>0.50</sub>P(20%) composite membrane



An improvement in the thermal stability, to a certain extent, of the nanocomposites can be noticed. All weight losses leaving residues. The amount of residue content found to be depend on nature of the resultant composite membrane. The inorganic material found to be well dispersed in the organic matrix.

## 4. Conclusion

Novel nanosized layered  $\alpha\text{-Hf}(\text{HPO}_4)_2\cdot\text{H}_2\text{O}(\text{nHfP})$ ,  $\alpha\text{-Hf}_x\text{Ti}_{(1-x)}(\text{HPO}_4)_2\cdot\text{H}_2\text{O}(\text{nHfTiP})$ , (where  $x = 0.9, 0.67, 0.50$ ) were prepared from crystallization of their parent glassy sodium forms with HF solution in Pyrex glass. Their average diameter found to be 10.15, 18.69, 18.69, 16.92 nm, respectively. We think these materials crystallized during the conversion process in two steps: 1<sup>st</sup> their parent glassy sodium forms dissolved in HF solution forming a mixing complex, 2<sup>nd</sup> the crystalline products were gradually precipitated due to HF solution action on the Pyrex flask and to a certain extent evaporation of excess HF. This will explain the formation of high degree of crystallinity of the resulting layered materials. These materials can be considered new inorganic ion exchangers, proton conductance and as solid acid catalysts.

Series novel polystyrene / (nHfP)-, (nHfTiP) nanocomposite membranes were obtained from PS solution with different weight percentages of the inorganic material (10, 20% in wt), respectively. The results indicated that inorganic material possesses good miscibility which lead to the formation of homogeneous transparent flexible thin films. Lead to the improvement of the thermal stability and mechanical properties, that may combine physical properties and characteristics of both organic and inorganic components within the single composite. The amount of residues obtained from TGA analysis ranges from 4-13 % in wt. These composites are promising for utilizations in fuel cells and as new sorbents.

## Acknowledgement

Authors are thankful To Department of Chemistry, Faculty of Science, University of Tripoli, Libya, for providing facilities for this research.

## References

- [1] Thakar, R. and Chudasama, U., 2009. "Synthesis, characterization proton transport of crystalline zirconium-titanium phosphates." *J. of Sci. and Ind. Res.*, vol. 68, p. 312-318.
- [2] Alberti, G., Cherubini, F., and Palombari, R., 1996. "Preparation, proton transport and use in gas sensors of thin film zirconium phosphate with  $\gamma$ -layered structure." *Sensors and Actuators*, vol. 2, p. 179.
- [3] Clearfield, A., 1993. "Ion exchange and adsorption in layered phosphates." *Mater. Chem. and Phys.*, vol. 257,
- [4] Colon, J. L., Diaz, A., and Clearfield, A., 2010. "Nanoincapsulation of insulin into zirconium phosphate for oral delivery applications." *Biomacromolecules*, vol. 9, p. 2465.
- [5] Bauer, F. and Porada, M. W., 2006. "Comparison between nafion and a nafion zirconium phosphate nanocomposite in fuel cell application." *Fuel Cells*, vol. 6, p. 261.
- [6] Diaz, A., Saxena, V., Gonzalez, J., David, A., Casanas, B., Carpenter, C., Batteas, J. D., Colon, J., Clearfield, A., *et al.*, 2012. "Zirconium phosphate nano-platelets: a novel platform for drug delivery in cancer therapy." *Chem Commun*, vol. 48, p. 1754.
- [7] Alberti, G., Casciola, M., Captani, D., Donnadio, A., Narducci, R., Pica, M., and Sganappa, M. N., 2007. "Novel nafion-zirconium phosphate composite membranes with enhanced stability of proton conductivity." *Electrochimica Acta*, vol. 52, p. 8125.

- [8] Yang, Y., Liu, C., and Wen, H., 2009. "Preparation and properties of polyvinyl alcohol / exfoliated  $\alpha$ -zirconium phosphate." vol. 28, p. 185.
- [9] Nagarale, R. K., Shin, W., and Singh, P. K., 2010. "Progress in ionic organic-inorganic composite membranes for fuel cell application." *Polym. Chem.*, vol. 1, p. 388.
- [10] Shakshooki, S. K., Elejmi, A. A., Khalfulla, A. M., and Elfituri, S. S., 2010. "Poly- (vinylalcohol)/ Lamellar titanium phosphate nanocomposite membranes." In *Int. Conf. on Mater. Imperative Cairo, Egypt* pp. 49-70.
- [11] Feng, Y., He, W., Zhang, X., Jia, X., and Zhao, H., 2007. "The preparation of nanoparticle zirconiumphosphate." *Mater. Letters*, vol. 61, p. 3258.
- [12] Bao, C., Gua, Y., Song, L., Lu, H., Yuan, B., and Hu, Y., 2011. "Facile synthesis of poly(vinylalcohol)/ $\alpha$ -titanium phosphate nanocomposite with markedly enhanced properties." *Ind. Eng. Chem. Res.*, vol. 50, p. 11109.
- [13] Yang, C. C., Chiu, S. J., and Chien, W. C., 2006. "Development of alkaline direct methanol fuel cells based on crosslinked PVA polymer membranes." *J. Power Sources*, vol. 162, p. 21.
- [14] Helen, M., Viswanathan, B., and Murthy, S. S., 2010. "Poly(vinyl alcohol)-polyacrylamide blends with cesium salts of heteropolyacid as a polymer electrolyte for direct methanol fuel cell applications." *J. Appl. Polym. Sci.*, vol. 116, p. 3437.
- [15] Paralikara, S. A., Simonsen, J., and Lombardi, J., 2008. "Poly(vinyl alcohol) /cellulose nanocrystal barrier membranes." *J. Membr. Sci.*, vol. 320, p. 248.
- [16] Sullad, A. G., Manjeshwar, L. S., and Aminabhavi, T. M., 2010. "Polymericblend microspheres for controlled release of the ophylline." *J. Appl. Polym. Sci.*, vol. 117, p. 1361.
- [17] Salavagione, H. J., Martinez, G., and Gomez, M. A., 2010. "Synthesis of poly(vinylalcohol) /reduced graphite oxide nanocomposites with improved thermal and electrical properties." *J. Mater.Chem.*, vol. 19, p. 5027.
- [18] Zang, R. and Hu, Y., 2011. "Onlie, Solvo thermal synthesis of organically modified  $\alpha$ -zirconium phosphate based polystyrene." *DO*, vol. 10, p. 1002.
- [19] Shakshooki, S. K., El-Mismary, Y., Dehair, A., Szirtes, L., Pavlovski, L., and Poko, Z., 1993. "Thermal decomposition of amorphous mixed glassy type hafnium-titanium phosphates." *J. Therm. Anal.*, vol. 39, p. 817.
- [20] Allen, T., 1992. *Particle sizes measurements*. 3rd ed. London: Chapman and Hall.
- [21] Shakshooki, S. K., Azzabi, O. H., Khalil, S., Kowalczyk, J., and Naqvi, N., 1988. "Crystalline mixed hafnium-titanium phosphates." *Reactive Polymers*, vol. 7, p. 191.
- [22] Shakahooki, S. K., El-Azzabi, O. H., Turki, F. M., El-Akari, F. A., Abodlal, S. A., and El-Tarhuni, S. R., 2012. "FT-IR and thermal behavior of  $\theta$ -type zirconium- and hafnium phosphates and their pellicular membranes." *Egypt J. Anal. Chem.*, vol. 12, p. 45.